HHS Public Access

Author manuscript

Wiley Interdiscip Rev Nanomed Nanobiotechnol. Author manuscript; available in PMC 2017 July 01.

Published in final edited form as:

Wiley Interdiscip Rev Nanomed Nanobiotechnol. 2016 July ; 8(4): 619–630. doi:10.1002/wnan.1386.

Engineering of Radiolabeled Iron Oxide Nanoparticles for Dual-Modality Imaging

Fanrong Ai,
School of Mechanical & Electrical Engineering, Nanchang University, Jiangxi, China

Department of Radiology, University of Wisconsin – Madison, WI, USA

Carolina A. Ferreira,
Department of Biomedical Engineering, University of Wisconsin–Madison, WI, USA

Feng Chen, and
Department of Radiology, University of Wisconsin – Madison, WI, USA

Weibo Cai
Department of Radiology, University of Wisconsin – Madison, WI, USA

Department of Medical Physics, University of Wisconsin – Madison, WI, USA

Department of Biomedical Engineering, University of Wisconsin – Madison, WI, USA

University of Wisconsin Carbone Cancer Center, Madison, WI, USA

Feng Chen: fchen@uwhealth.org; Weibo Cai: wcai@uwhealth.org

Abstract

Over the last decade, radiolabeled iron oxide nanoparticles have been developed as promising contrast agents for dual-modality positron emission tomography/magnetic resonance imaging (PET/MRI) or single-photon emission computed tomography/magnetic resonance imaging (SPECT/MRI). The combination of PET (or SPECT) with MRI can offer synergistic advantages for non-invasive, sensitive, high-resolution, and quantitative imaging, which is suitable for early detection of various diseases such as cancer. Here, we summarize the recent advances on radiolabeled iron oxide nanoparticles for dual-modality imaging, through the use of a variety of PET (and SPECT) isotopes by using both chelator-based and chelator-free radiolabeling techniques.

INTRODUCTION

Molecular imaging, “the visualization, characterization and measurement of biological processes at the molecular and cellular levels in humans and other living systems”,[1] have enabled the visualization of specific molecular events in disease processes and have made great progress in modern diagnostics.[2, 3] In general, molecular imaging modalities include optical bioluminescence (or optical fluorescence), ultrasound, magnetic resonance imaging

Correspondence to: Feng Chen, fchen@uwhealth.org; Weibo Cai, wcai@uwhealth.org.

Conflict of interest: The authors have declared no conflicts of interest for this article.

(MRI), magnetic resonance spectroscopy (MRS), single-photon emission computed tomography (SPECT), and positron emission tomography (PET).[4–6] MRI and PET are two of the most important imaging modalities that are used in daily clinical disease diagnosis. MRI is well-known for providing unmatched soft tissue details, however, suffers from relatively low sensitivity.[7] The radionuclide-based SPECT and PET imaging are highly sensitive and quantitative nuclear imaging technologies, which share the same limitations of low spatial resolution. Modern PET and SPECT scanners all come with computed tomography (CT), where functional imaging obtained by PET and SPECT (which depicts the spatial distribution of metabolic or biochemical activity in the body) can be more precisely aligned or correlated with anatomic imaging obtained by CT scanning. PET/MRI is a raising hybrid imaging technology that incorporates MRI soft tissue morphological imaging and PET functional imaging (which can not be achieved by using PET or PET/CT alone) and is believed to play a vital role in clinical fields, such as oncology, cardiology, and neurology.[8, 9] The first MRI-compatible PET system was reported in 2008 by using lutetium oxyorthosilicate scintillation crystals and avalanche photodiodes as PET detector.[10] Unlike the conventional PET/CT where imaging information is acquired sequentially, PET/MRI can be performed simultaneous, leading to greatly improve the diagnostic potential.[11] Readers are referred to excellent reviewer articles in regards to PET/MRI system design.[12–15]

Radiolabeled iron oxide nanoparticles have attracted great attention recently due to their ability to act both as MRI contrast agent and PET (or SPECT) imaging tracer, making them well-suited probes for dual-modality tumor imaging.[16] Herein, we introduce recent advances in the engineering of radiolabeled iron oxide nanoparticles for PET/MRI and SPECT/MRI dual-modality imaging. A wide range of PET and SPECT isotopes and their radiolabeling techniques will be discussed.

CATEGORIES OF RADIOLABELED IRON OXIDE NANOPARTICLES

Iron oxide nanoparticle (IONP) is a T_2-weighted MRI contrast agent, which can shorten the T_2 relaxation time of water.[17] The last decade has witnessed great advances of engineering of various kinds of magnetic iron oxide nanoparticles for MR imaging.[18, 19] For example, cube-shaped iron oxide nanoparticles (IONPs) with a particle size of ~22 nm have been developed and showed an extremely high r_2 relaxivity (>700 $mM^{-1}s^{-1}$).[20] Besides, decorating of IONPs over other nanoplatforms, such as silica or polymers, has been considered to be an alternative method to improve the r_2 value.[21, 22] Large-scale synthesis of uniform and extremely small-sized (<4 nm) iron oxide nanoparticles has also been reported for high-resolution T_1-weighted MR imaging.[23] Novel contrast agents for both nuclear and MR imaging can be achieved by labeling a variety of SPECT isotopes (such as ^{99m}Tc, ^{123}I or ^{125}I, ^{111}In, *etc.*), and PET isotopes (such as ^{18}F, ^{11}C, ^{64}Cu, ^{68}Ga, ^{69}Ge, ^{89}Zr, ^{72}As, *etc.*) to water-soluble iron oxide nanoparticles.

Chelator-based Synthesis of Radiolabeled Iron Oxide Nanoparticles

The most widely used radiolabeling strategy involves the use of exogenous chelators which could coordinate with certain radioisotopes to form stable complexes.[24, 25] Different isotopes vary significantly in their coordination chemistry, making selection of the right

chelator for a specific isotope vital. In this section, radiolabeled IONPs synthesized with the assistance of various kinds of chelators will be discussed.

^{99m}Tc-labeled Iron Oxide Nanoparticles

The most commonly used radionuclide in SPECT is Technetium-99m (^{99m}Tc, $t_{1/2}$=6 h).[20] Successful labeling of ^{99m}Tc to nanoparticles is based on the fact that the reduced $^{99m}TcO_4^-$ ($SnCl_2$ is usually the reducing agent) can react with an electron donor group, such as the group $–COO^-$ from diethylene triamine pentaacetic acid (DTPA) and 1,4,7-triazacyclononane-triacetic acid (NOTA), or the group $–NH_2$ from chitosan, to form a ^{99m}Tc-chelate.[26] For example, Madru *et al.* prepared ^{99m}Tc-labeled IONPs for multimodality SPECT/MRI imaging of sentinel lymph nodes.[27] The labeling method described in this work was simple and straightforward. When the oxidation state of $^{99m}TcO_4^-$ is reduced with a stannous chloride solution, ^{99m}Tc binds to the functionalized polyethylene glycol (PEG) coating from the IONP surface. The radiolabeling yield was found to be 99% with high radiostability in both sterile water and human serum. ^{99m}Tc-IONPs uptake in the SLN was found to be more than 200 %ID/g, whereas it was less than 2 %ID/g in liver and spleen. Results further indicated that ^{99m}Tc-IONPs can be detected with both imaging techniques, and can act as multimodality contrast agents for sentinel lymph node mapping. ^{99m}Tc-labeled NOTA-IONPs polymer-shelled microbubbles (MBs) and DTPA-IONPs MBs have also been developed for monitoring the distribution and clearance of nanoparticles in vivo.[26]

A new class of dual-modality imaging agents based on the conjugation of radiolabeled bisphosphonates (BP) directly to the surface of ultrasmall superparamagnetic iron oxide (USPIO) nanoparticles have also been reported.[28, 29] For example, researchers have prepared ^{99m}Tc-PEG-BP-USPIO for T_1-weighted MRI-SPECT multimodal imaging (Figure 1A).[29] *In vitro* MRI studies showed that as-designed nanoparticles have a high r_1 with a low r_2/r_1 ratio of 9.5 mM^{-1} s^{-1} and 2.97, respectively. When compared with non-functionalized USPIO, the new contrast agent showed a similar signal enhancement by using four times lower dose. The nanoparticles also showed long blood circulation time ($t_{1/2}$=2.97 h), allowing the visualization of blood vessels and vascular organs with high spatial definition (Figure 1B). ^{99m}Tc-labeled and Bevacizumab monoclonal antibody (mAb) conjugated USPIO (^{99m}Tc-USPIO-bevacizumab) was also synthesized for targeted imaging of hepatocellular carcinoma.[30] Although therapeutic applications of radiolabeled iron oxide nanoparticle is not the main focus of this article, reports on engineering of these nanoparticles for combined magnetic hyperthermia (or radiation therapy) have shown their potential as novel theranostic nanoagents for both multimodality imaging and therapy.[31–33]

^{111}In- and ^{125}I-labeled Iron Oxide Nanoparticles

Indium-111 (^{111}In, $t_{1/2}$=2.8 d) is another radionuclide in clinical nuclear medicine for its reasonably long half-life. Misri *et al.* developed a dual-modality molecular imaging probe by conjugating ^{111}In-labeled antimesothelin antibody mAbMB (i.e.^{111}In-mAbMB) to IONPs.[34] DTPA was used the chelator for ^{111}In labeling. IONPs were coated with carboxy methyl dextran, providing carboxylic acid groups for the ^{111}In-mAbMB antibody conjugation. *In*

vivo SPECT and MRI dual-modality imaging was carried out on A431K5 tumor-bearing mice. Specific uptake of ^{111}In-mAbMB-IONPs in A431K5 tumor (mesothelin-positive tumor model, 4.8 %ID/g) was found significantly higher than the non-specific accumulation in A431 tumor (mesothelin-negative tumor model, 2.7 %ID/g). Although a much higher uptake in spleen (up to 68 %ID/g) was observed in the study, the combination of SPECT with MRI holds the potential to obtain both functional and anatomical imaging information with high signal sensitivity and contrast, thereby providing a powerful diagnostic tool for early diagnosis and treatment planning of mesothelin-expressing cancers in the future.

In another study, ^{111}In-labeled, and chimeric L6 (ChL6), a human–mouse mAb chimera, conjugated IONPs were developed for pharmacokinetics, tumor active targeting, and alternating magnetic frequency (AMF) therapy studies.[35] Tumor uptake was detected to be about 14 %ID/g at 48 h post injection. External AFM was applied on the injected mice and magnetic hyperthermia tumor toxicity studies were carried out. Results showed tumor growth delay in all groups, except for the group with the lowest heat dose. Electron microscopy further confirmed the presence of necrosis after AMF treatment. This was one of the few reports that showed the potential of using radiolabeled INOPs for tumor targeted thermal therapy. IONPs labeled with ^{111}In, iron-59 (^{59}Fe, $t_{1/2}$=49.5 d) and carbon-14 (^{14}C, $t_{1/2}$=5700 y) have also been reported for evaluating the in vivo integrity of radiolabeled IONPs.[36]

Radioisotopes of iodine have been extensively used in clinical nuclear medicine imaging and radiation therapy. There are 37 known isotopes of iodine from ^{108}I to ^{144}I, and four of those, ^{123}I, ^{124}I, ^{125}I and ^{131}I, are suitable for SPECT or PET imaging. Tang and co-workers synthesized a SPECT/MRI/optical trimodality probe by labeling fluorescent silica coated IONPs with iodine-125.[37] ^{125}I-labeling was achieved by the Iodogen oxidation method. This novel probe was used to label mesenchymal stem cells (MSCs) and quantitatively track their migration and biodistribution in ischemic rats. As-developed nanoprobes showed high labeling efficiency and could allow *in vivo* tracking of labeled MSC with high spatial resolution and anatomical localization through SPECT and MRI imaging. The long half-life (59 d) of ^{125}I also enabled a long-term tracking and imaging of the labeled cells. No detection limitation was reported in this study.

^{64}Cu- and ^{68}Ga-labeled Iron Oxide Nanoparticles

When compared with SPECT imaging, PET imaging may offer increased accuracy, higher sensitivity and better resolution.[38] Hybrid imaging of high-resolution anatomical MRI and PET might offer an even better solution for future early cancer diagnosis. Copper-64 (^{64}Cu, $t_{1/2}$=12.7 h) is a positron emitter with a reasonably long half-life and well-established radiolabeling techniques. Chelators, such as DTPA, NOTA, 1,4,7,10-tetraazacyclododecane-1,4,7,10-tetraacetic acid (DOTA), and bis-dithiocarbamatebisphosphonate (DTCPB) have been used for the radiolabeling of ^{64}Cu to INOPs for PET/MRI dual-modality imaging.[39, 40]

For example, a novel amine-activated chelator (amine-Bz-DOTA) was developed and conjugated to the surface of dextran sulfate coated IONPs for ^{64}Cu radiolabeling.[40] The new

labeling procedure was able to avoid the cross-link of IONPs (which caused nanoparticles aggregation) and enabled a higher labelling yield. By using NOTA as the chelator, we also developed a ^{64}Cu-labeled, cRGD-functionalized, and therapeutic drug doxorubicin (DOX)-conjugated IONPs for drug delivery and PET/MRI imaging (Figure 2A, B).[41] Enhanced and specific accumulation of cRGD-conjugated IONPs in U87MG tumor-bearing mice was demonstrated by using PET imaging (Figure 2C). In a similar study, Lee *et al.* developed a RGD-conjugated and ^{64}Cu-labeled iron oxide nanoparticles for PET/MRI dual-modality tumor imaging.[42] Both small-animal PET and T_2-weighted MR imaging show integrin-specific delivery of RGD-conjugated IONPs, together with prominent reticuloendothelial system uptake due to the large particle size (>40 nm). Quantitative PET imaging and region of interest analysis showed about 10.1 %ID/g in mice injected with ^{64}Cu-DOTA-IONPs-RGD conjugates at 4 h post injection, while tumor uptakes of the non-targeted and blocking groups were only 4 %ID/g and 3 %ID/g, respectively.

A more complex hetero-nanostructure with two different functional nanomaterials (i.e. gold and iron oxide) within one structure has been used as the platform for radiolabeling and targeted trimodality (PET/MRI/optical) imaging (Figure 3A).[43] As-synthesized hybrid nanoparticles have a dumbbell shape (Figure 3B, C), and can be further modified with PEG and chelators for prolonged blood circulation time and radiolabeling. Both *in vivo* PET and MRI demonstrated the specific targeting of anti-EGFR Affibody protein conjugated and ^{64}Cu-labeled hybrid nanoparticle, denoted as ^{64}Cu-NOTA-Au-IONP-Affibody (Figure 3D, E).

Gallium-68 (^{68}Ga, $t_{1/2}$= 68 min) can be easily synthesized using ^{68}Ge/^{68}Ga generators. Kim *et al.* reported a ^{68}Ga radiolabeled tumor-targeting IONPs, using NOTA as the radiolabeling chelator.[44] The authors used oleanolic acid (OA), a tumor-targeting molecule, to modify the IONPs, and then coupled it with NOTA for ^{68}Ga radiolabeling. The ^{68}Ga-NOTA-OA-IONPs were intravenously injected into HT29 tumor-bearing mice for *in vivo* PET/MRI imaging. The tumor uptake of ^{68}Ga-NOTA-OA-IONPs was found to be about 3 %ID/g. No non-targeted and blocking studies were provided to demonstrate the targeting specificity of ^{68}Ga-NOTA-OA-IONPs.

Although chelator-based radiolabeling techniques have been used for decades, concerns about the complexity of coordination chemistry, possible altering of pharmacokinetics of carriers, and potential detachment of radioisotopes during imaging have driven the need for developing a simpler yet better technique for future radiolabeling. There is an emerging concept of intrinsically radiolabeled nanoparticles, which can be synthesized using methods such as hot-plus-cold precursors, specific trapping, cation exchange and proton beam activation.[45, 46] In the next section, we will discuss radiolabeled IONPs using chelator-free method.

Chelator-free Synthesis of Radiolabeled Iron Oxide Nanoparticles

^{18}F- and ^{11}C-labeled Iron Oxide Nanoparticles

Fluorine-18 (^{18}F, $t_{1/2}$=109 min) is a widely available PET isotope. Devaraj *et al.* reported an ^{18}F-radiolabeled Vivotag-680 functionalized IONPs for multimodality imaging.[47] IONPs

were coated with aminated cross-linked dextran, which was functionalized first with near-infrared fluorochrome Vivotag-680. After that, ^{18}F-PEG was conjugated using copper-catalyzed azide-alkyne click chemistry, forming a trimodal nanoparticle (^{18}F-CLIO) that is suitable for multimodality imaging (PET, fluorescence and MRI). The radiochemical purity of ^{18}F-CLIO was detected to be >99% according to high-performance liquid chromatography analysis. Results also showed that the detection threshold of ^{18}F-CLIO for PET imaging was 200 times more sensitive than MRI. *In vivo* dynamic PET imaging showed high signal-to-noise ratios. Furthermore, ^{18}F-CLIO presented a vascular half-life of 5.8 h in mice and subsequent internalization into liver, spleen and phagocytic cells of other lymphatic organs. Another interesting chelator-free labeling method was reported by Cui and co-workers, who labeled ^{18}F to Fe_3O_4@$Al(OH)_3$ by taking advantages of the high affinity between $Al(OH)_3$ and fluoride anions.[48]

Carbon-11(^{11}C, $t_{1/2}$=20.3 min) is another non-metal isotope with a relatively short half-life that can be used for making ^{11}C-labeled IONPs.[49] In a study reported by Ramesh Sharma and co-workers, [^{11}C]CH_3I was used to react with carboxylic acid (–COOH) or amine (–NH_2) functional groups modified IONPs. Although the radiolabeling yield was lower than 3%, ^{11}C-labeled IONPs had sufficient radioactivity to perform PET imaging for short-term dynamics and biodistribution studies. The low radiolabeling yield was primarily due to INOPs agglomeration and low carboxylic acid or amine functional ligand density on the surface of nanoparticles. *In vivo* dual-modality PET/MRI of mouse showed an excellent correlation between PET and MRI data for the distributions of ^{11}C-labeled IONPs.

*As- and ^{69}Ge-labeled Iron Oxide Nanoparticles

Arsenic (As) has 4 positron emitting ($^{70/71/72/74}$As) and 3 electron emitting ($^{74/76/77}$As) radioisotopes with half-lives ranging from 52.6 min to 17.8 days, which could be useful for both PET and internal radiotherapy applications.[50] However, few techniques are currently available for incorporation of these radionuclides into biologically relevant targeting vectors. Inspired by an ancient groundwater decontamination process, where both As^{III} and As^{V} can be incorporated by magnetite or IONPs,[51–54] we demonstrated a simple but highly efficient strategy for the synthesis of radioarsenic-labeled IONPs (i.e. *As-IONP, *=71, 72, 74, 76) without the use of any chelators (Figure 4A). The underlying mechanism of arsenic trapping by IONP involves the formation of highly stable arsenic complexes, where $As^{III}O_3$ trigonal pyramids or $As^{V}O_4$ tetrahedra occupy vacant FeO_4 tetrahedral sites on the octahedrally terminated (111) surface of the magnetite nanoparticles.[55] Oleic acid capped IONPs were first synthesized and transfer to water phase by modifying with poly(acrylic acid) (PAA) (Figure 4B, C). The labeling of *As (*= 71, 72, 74, 76) to IONPs was later demonstrated to be fast, iron concentration dependent, and highly specific. Although the in vivo stability of *As-IONPs still needs to be improved, the PEGylated *As-IONPs showed improved serum stability and less bladder uptake *in vivo*. PET/MRI dual-modality lymph node mapping using *As-IONPs@PEG was also demonstrated *in vivo* (Figure 4D, E). Germanium-69, (^{69}Ge, $t_{1/2}$= 39.05 h) is another novel potential PET radioisotope, whose *in vivo* applications are hampered by its complex coordination chemistry in aqueous medium. To circumvent this challenge, we also exploited the high affinity of germanium for metal oxides to develop the first chelator-free ^{69}Ge-labeled IONPs based agent for PET/MRI lymph node mapping.[56]

64Cu- and ^{89}Zr-labeled Iron Oxide Nanoparticles

Besides labeling *As and ^{69}Ge to IONPs using specific trapping strategy, intrinsically ^{111}In-, ^{64}Cu-, iron-59 (^{59}Fe, $t_{1/2}$=44.5 d) labeled IONPs could also be synthesized by using hot-plus-cold precursors technique.[57–59] Recently, we further developed MoS_2-IONP nanosheets for ^{64}Cu chelator-free radiolabeling and multimodality image-guided photothermal therapy (PTT) (Figure 5A).[60] MoS_2-IONPs were prepared by self-assembling of IONPs on the surface of MoS_2 nanosheets *via* sulfur chemistry, and were PEGylated for improved *in vivo* stability (Figure 5B). ^{64}Cu could be easily labeled to the MoS_2-IONPs by taking advantages of the high affinity between $^{64}Cu^{2+}$ ions and sulfur atoms. Labeling yield was measured to be 85% at optimal experimental condition. PET imaging of as-developed ^{64}Cu-MoS_2-IONPs in 4T1 tumor-bearing mice showed about 6 %ID/g passive targeting efficacy (Figure 5C). *In vivo* MR imaging further confirmed the accumulation of nanoparticles in the tumor site (Figure 5D). We also demonstrated effective image-guided PTT by exposing the MoS_2-IONPs injected mice to an 808 nm laser. Enhanced PTT effect is also expected by further conjugating ^{64}Cu-MoS_2-IONPs with targeting ligands in follow-up studies.

Zirconium-89 (^{89}Zr, $t_{1/2}$=78.4 h) is a radioisotope with a relatively low positron energy (β^+_{avg}=395.5 keV), making it highly suitable for long blood circulating monoclonal antibody-based PET imaging.[61] Desferrioxamine (DFO), a hexadentate ligand with three hydroxamate groups that provide six oxygen donors for metal binding, is currently the preferred chelator for labeling of ^{89}Zr.[62] For example, ^{89}Zr-DFO-ferumoxytol was developed for PET/MRI mapping of deep-tissue lymph nodes in live animals.[63] Recently, a chelater-free iron bonding and heat-induced radiolabeling of IONPs was also developed.[64] Holland and co-workers demonstrated that ferumoxytol could be labeled with the ^{89}Zr, ^{64}Cu and ^{111}In under the similar general reaction conditions (i.e. 120 °C under pH 8) without using any chelates.[64] *In vivo* pharmacokinetics and distribution of ^{89}Zr-ferumoxytol nanoparticles were preformed using PET/CT imaging, and showed the circulating of radiolabeled nanoparticles in the blood during as well as high liver and spleen uptake in the mice. As-developed labeling strategy might also apply to other metal or non-metal oxide nanoparticles.

SUMMARY AND OUTLOOK

In conclusion, radiolabeled IONPs have emerged as a novel dual-modality contrast agents which already shown their potential for providing non-invasive, high-resolution and quantitative imaging results. Table 1 further provides a collection of representative radiolabeled IONPs *via* different radiolabeling methods. Despite the progress that has been made in the last decade, challenges still exist for engineering of radiolabeled IONPs for future dual-modality imaging and clinical translation.

Firstly, most of radiolabeled IONPs reviewed in this article have hydrodynamic size range of 10 to 200 nm, which caused high and retained accumulation in the reticuloendothelial system (RES) organs. Considering the fact that the Food and Drug Administration requires all injected contrast agents to be cleared completely within a reasonable period,[65, 66] engineering of radiolabeled IONPs that can be cleared by the renal system will be one of the

next major focuses. Secondly, specific delivery of the radiolabeled IONPs to tumor site is critical for dual-modality imaging. Engineering of tumor actively targeted radiolabeled IONPs is still in its early stage with only a few examples being reported. Thirdly, due to the lack of accessibility to the PET/MRI scanners, most of current PET and MRI images were acquired separately. The true advantages of simultaneously PET/MRI in early cancer diagnosis using radiolabeled IONPs are believed to be further revealed in the near future.

ACKNOWLEDGEMENT

This work was supported, in part, by the University of Wisconsin - Madison, the National Institutes of Health (NIBIB/NCI R01CA169365, P30CA014520), the American Cancer Society (125246-RSG-13-099-01-CCE), the National Natural Science Foundation of China (51102131), the National Natural Science Foundation of Jiangxi Province, China (20142BAB216033) and a Science without Borders Ph.D. Program scholarship from Brazil.

REFERENCES

1. Mankoff DA. A Definition of Molecular Imaging. Journal of Nuclear Medicine. 2007; 48:18N–21N.
2. Hoffman JM, Gambhir SS. Molecular imaging: The vision and opportunity for radiology in the future. Radiology. 2007; 244:39–47. [PubMed: 17507723]
3. Lee S, Xie J, Chen X. Activatable molecular probes for cancer imaging. Curr Top Med Chem. 2010; 10:1135–1144. [PubMed: 20388112]
4. Cai W, Chen X. Multimodality Molecular Imaging of Tumor Angiogenesis. Journal of Nuclear Medicine. 2008; 49:113S–128S. [PubMed: 18523069]
5. Key J, Leary JF. Nanoparticles for multimodal in vivo imaging in nanomedicine. International Journal of Nanomedicine. 2014; 9:711–726. [PubMed: 24511229]
6. Rieffel J, Chitgupi U, Lovell JF. Recent Advances in Higher-Order, Multimodal, Biomedical Imaging Agents. Small. 2015; 11:4445–4461. [PubMed: 26185099]
7. Mahmoudi M, Hosseinkhani H, Hosseinkhani M, Boutry S, Simchi A, Journeay WS, Subramani K, Laurent S. Magnetic resonance imaging tracking of stem cells in vivo using iron oxide nanoparticles as a tool for the advancement of clinical regenerative medicine. Chem Rev. 2011; 111:253–280. [PubMed: 21077606]
8. Partovi S, Kohan A, Rubbert C, Vercher-Conejero JL, Gaeta C, Yuh R, Zipp L, Herrmann KA, Robbin MR, Lee Z, et al. Clinical oncologic applications of PET/MRI: a new horizon. Am J Nucl Med Mol Imaging. 2014; 4:202–212. [PubMed: 24753986]
9. Hu Z, Yang W, Liu H, Wang K, Bao C, Song T, Wang J, Tian J. From PET/CT to PET/MRI: advances in instrumentation and clinical applications. Mol Pharm. 2014; 11:3798–3809. [PubMed: 25058336]
10. Schlemmer HP, Pichler BJ, Schmand M, Burbar Z, Michel C, Ladebeck R, Jattke K, Townsend D, Nahmias C, Jacob PK, et al. Simultaneous MR/PET imaging of the human brain: feasibility study. Radiology. 2008; 248:1028–1035. [PubMed: 18710991]
11. Judenhofer MS, Wehrl HF, Newport DF, Catana C, Siegel SB, Becker M, Thielscher A, Kneilling M, Lichy MP, Eichner M, et al. Simultaneous PET-MRI: a new approach for functional and morphological imaging. Nat Med. 2008; 14:459–465. [PubMed: 18376410]
12. Roncali E, Cherry SR. Application of silicon photomultipliers to positron emission tomography. Ann Biomed Eng. 2011; 39:1358–1377. [PubMed: 21321792]
13. Delso G, Ziegler S. PET/MRI system design. Eur J Nucl Med Mol Imaging. 2009; 36(Suppl 1):S86–S92. [PubMed: 19104809]
14. Zaidi H, Del Guerra A. An outlook on future design of hybrid PET/MRI systems. Med Phys. 2011; 38:5667–5689. [PubMed: 21992383]
15. Judenhofer MS, Cherry SR. Applications for preclinical PET/MRI. Semin Nucl Med. 2013; 43:19–29. [PubMed: 23178086]
16. Lee DE, Koo H, Sun IC, Ryu JH, Kim K, Kwon IC. Multifunctional nanoparticles for multimodal imaging and theragnosis. Chem Soc Rev. 2012; 41:2656–2672. [PubMed: 22189429]

17. Amanlou M, Siadat SD, Norouzian D, Ebrahimi SE, Aghasadeghi MR, Ghorbani M, Alavidjeh MS, Inanlou DN, Arabzadeh AJ, Ardestani MS. Magnetic resonance contrast media sensing in vivo molecular imaging agents: an overview. Curr Radiopharm. 2011; 4:31–43. [PubMed: 22191613]
18. Ling D, Lee N, Hyeon T. Chemical synthesis and assembly of uniformly sized iron oxide nanoparticles for medical applications. Acc Chem Res. 2015; 48:1276–1285. [PubMed: 25922976]
19. Ling D, Hyeon T. Chemical design of biocompatible iron oxide nanoparticles for medical applications. Small. 2013; 9:1450–1466. [PubMed: 23233377]
20. Lee N, Choi Y, Lee Y, Park M, Moon WK, Choi SH, Hyeon T. Water-dispersible ferrimagnetic iron oxide nanocubes with extremely high R2) relaxivity for highly sensitive in vivo MRI of tumors. Nano Lett. 2012; 12:3127–3131. [PubMed: 22575047]
21. Laurent S, Forge D, Port M, Roch A, Robic C, Vander Elst L, Muller RN. Magnetic iron oxide nanoparticles: synthesis, stabilization, vectorization, physicochemical characterizations, and biological applications. Chem Rev. 2008; 108:2064–2110. [PubMed: 18543879]
22. Lee JE, Lee N, Kim H, Kim J, Choi SH, Kim JH, Kim T, Song IC, Park SP, Moon WK, et al. Uniform mesoporous dye-doped silica nanoparticles decorated with multiple magnetite nanocrystals for simultaneous enhanced magnetic resonance imaging, fluorescence imaging, and drug delivery. J Am Chem Soc. 2010; 132:552–557. [PubMed: 20017538]
23. Kim BH, Lee N, Kim H, An K, Park YI, Choi Y, Shin K, Lee Y, Kwon SG, Na HB, et al. Large-scale synthesis of uniform and extremely small-sized iron oxide nanoparticles for high-resolution T1 magnetic resonance imaging contrast agents. J Am Chem Soc. 2011; 133:12624–12631. [PubMed: 21744804]
24. Liu S. Bifunctional coupling agents for radiolabeling of biomolecules and target-specific delivery of metallic radionuclides. Adv Drug Deliv Rev. 2008; 60:1347–1370. [PubMed: 18538888]
25. Sarko D, Eisenhut M, Haberkorn U, Mier W. Bifunctional chelators in the design and application of radiopharmaceuticals for oncological diseases. Curr Med Chem. 2012; 19:2667–2688. [PubMed: 22455579]
26. Barrefelt AA, Brismar TB, Egri G, Aspelin P, Olsson A, Oddo L, Margheritelli S, Caidahl K, Paradossi G, Dahne L, et al. Multimodality imaging using SPECT/CT and MRI and ligand functionalized 99mTc-labeled magnetic microbubbles. EJNMMI Res. 2013; 3:12. [PubMed: 23442550]
27. Madru R, Kjellman P, Olsson F, Wingardh K, Ingvar C, Stahlberg F, Olsrud J, Latt J, Fredriksson S, Knutsson L, et al. 99mTc-labeled superparamagnetic iron oxide nanoparticles for multimodality SPECT/MRI of sentinel lymph nodes. J Nucl Med. 2012; 53:459–463. [PubMed: 22323777]
28. Torres Martin de Rosales R, Tavare R, Glaria A, Varma G, Protti A, Blower PJ. ((9)(9)m)Tc-bisphosphonate-iron oxide nanoparticle conjugates for dual-modality biomedical imaging. Bioconjug Chem. 2011; 22:455–465. [PubMed: 21338098]
29. Sandiford L, Phinikaridou A, Protti A, Meszaros LK, Cui X, Yan Y, Frodsham G, Williamson PA, Gaddum N, Botnar RM, et al. Bisphosphonate-anchored PEGylation and radiolabeling of superparamagnetic iron oxide: long-circulating nanoparticles for in vivo multimodal (T1 MRI-SPECT) imaging. ACS Nano. 2013; 7:500–512. [PubMed: 23194247]
30. Zhao Y, Yao Q, Tan H, Wu B, Hu P, Wu P, Gu Y, Zhang C, Cheng D, Shi H. Design and preliminary assessment of 99mTc-labeled ultrasmall superparamagnetic iron oxide-conjugated bevacizumab for single photon emission computed tomography/magnetic resonance imaging of hepatocellular carcinoma. J Radioanal Nucl Chem. 2013; 299:1273–1280.
31. Baldi G, Ravagli C, Mazzantini F, Loudos G, Adan J, Masa M, Psimadas D, Fragogeorgi EA, Locatelli E, Innocenti C, et al. In vivo anticancer evaluation of the hyperthermic efficacy of anti-human epidermal growth factor receptor-targeted PEG-based nanocarrier containing magnetic nanoparticles. Int J Nanomedicine. 2014; 9:3037–3056. [PubMed: 25028545]
32. Tsiapa I, Efthimiadou EK, Fragogeorgi E, Loudos G, Varvarigou AD, Bouziotis P, Kordas GC, Mihailidis D, Nikiforidis GC, Xanthopoulos S, et al. (99m)Tc-labeled aminosilane-coated iron oxide nanoparticles for molecular imaging of alphanubeta3-mediated tumor expression and feasibility for hyperthermia treatment. J Colloid Interface Sci. 2014; 433:163–175. [PubMed: 25128864]

33. Psimadas D, Baldi G, Ravagli C, Comes Franchini M, Locatelli E, Innocenti C, Sangregorio C, Loudos G. Comparison of the magnetic, radiolabeling, hyperthermic and biodistribution properties of hybrid nanoparticles bearing CoFe2O4 and Fe3O4 metal cores. Nanotechnology. 2014; 25:025101. [PubMed: 24334365]
34. Misri R, Meier D, Yung AC, Kozlowski P, Hafeli UO. Development and evaluation of a dual-modality (MRI/SPECT) molecular imaging bioprobe. Nanomedicine. 2012; 8:1007–1016. [PubMed: 22100757]
35. DeNardo SJ, DeNardo GL, Natarajan A, Miers LA, Foreman AR, Gruettner C, Adamson GN, Ivkov R. Thermal dosimetry predictive of efficacy of 111In-ChL6 nanoparticle AMF--induced thermoablative therapy for human breast cancer in mice. J Nucl Med. 2007; 48:437–444. [PubMed: 17332622]
36. Wang H, Kumar R, Nagesha D, Duclos RI Jr, Sridhar S, Gatley SJ. Integrity of (111)In-radiolabeled superparamagnetic iron oxide nanoparticles in the mouse. Nucl Med Biol. 2015; 42:65–70. [PubMed: 25277378]
37. Tang Y, Zhang C, Wang J, Lin X, Zhang L, Yang Y, Wang Y, Zhang Z, Bulte JW, Yang GY. MRI/SPECT/Fluorescent Tri-Modal Probe for Evaluating the Homing and Therapeutic Efficacy of Transplanted Mesenchymal Stem Cells in a Rat Ischemic Stroke Model. Adv Funct Mater. 2015; 25:1024–1034. [PubMed: 26290659]
38. Rahmim A, Zaidi H. PET versus SPECT: strengths, limitations and challenges. Nucl Med Commun. 2008; 29:193–207. [PubMed: 18349789]
39. Glaus C, Rossin R, Welch MJ, Bao G. In vivo evaluation of (64)Cu-labeled magnetic nanoparticles as a dual-modality PET/MR imaging agent. Bioconjug Chem. 2010; 21:715–722. [PubMed: 20353170]
40. Jarrett BR, Gustafsson B, Kukis DL, Louie AY. Synthesis of 64Cu-labeled magnetic nanoparticles for multimodal imaging. Bioconjug Chem. 2008; 19:1496–1504. [PubMed: 18578485]
41. Yang X, Hong H, Grailer JJ, Rowland IJ, Javadi A, Hurley SA, Xiao Y, Yang Y, Zhang Y, Nickles RJ, et al. cRGD-functionalized, DOX-conjugated, and (6)(4)Cu-labeled superparamagnetic iron oxide nanoparticles for targeted anticancer drug delivery and PET/MR imaging. Biomaterials. 2011; 32:4151–4160. [PubMed: 21367450]
42. Lee HY, Li Z, Chen K, Hsu AR, Xu C, Xie J, Sun S, Chen X. PET/MRI dual-modality tumor imaging using arginine-glycine-aspartic (RGD)-conjugated radiolabeled iron oxide nanoparticles. J Nucl Med. 2008; 49:1371–1379. [PubMed: 18632815]
43. Yang M, Cheng K, Qi S, Liu H, Jiang Y, Jiang H, Li J, Chen K, Zhang H, Cheng Z. Affibody modified and radiolabeled gold-iron oxide hetero-nanostructures for tumor PET, optical and MR imaging. Biomaterials. 2013; 34:2796–2806. [PubMed: 23343632]
44. Kim SM, Chae MK, Yim MS, Jeong IH, Cho J, Lee C, Ryu EK. Hybrid PET/MR imaging of tumors using an oleanolic acid-conjugated nanoparticle. Biomaterials. 2013; 34:8114–8121. [PubMed: 23932293]
45. Sun X, Cai W, Chen X. Positron emission tomography imaging using radiolabeled inorganic nanomaterials. Acc Chem Res. 2015; 48:286–294. [PubMed: 25635467]
46. Goel S, Chen F, Ehlerding EB, Cai W. Intrinsically radiolabeled nanoparticles: an emerging paradigm. Small. 2014; 10:3825–3830. [PubMed: 24978934]
47. Devaraj NK, Keliher EJ, Thurber GM, Nahrendorf M, Weissleder R. 18F labeled nanoparticles for in vivo PET-CT imaging. Bioconjug Chem. 2009; 20:397–401. [PubMed: 19138113]
48. Cui X, Belo S, Kruger D, Yan Y, de Rosales RT, Jauregui-Osoro M, Ye H, Su S, Mathe D, Kovacs N, et al. Aluminium hydroxide stabilised MnFe2O4 and Fe3O4 nanoparticles as dual-modality contrasts agent for MRI and PET imaging. Biomaterials. 2014; 35:5840–5846. [PubMed: 24768194]
49. Sharma R, Xu Y, Kim SW, Schueller MJ, Alexoff D, Smith SD, Wang W, Schlyer D. Carbon-11 radiolabeling of iron-oxide nanoparticles for dual-modality PET/MR imaging. Nanoscale. 2013; 5:7476–7483. [PubMed: 23832243]
50. Cutler CS, Hennkens HM, Sisay N, Huclier-Markai S, Jurisson SS. Radiometals for combined imaging and therapy. Chem Rev. 2013; 113:858–883. [PubMed: 23198879]

51. Yavuz CT, Mayo JT, Yu WW, Prakash A, Falkner JC, Yean S, Cong L, Shipley HJ, Kan A, Tomson M, et al. Low-field magnetic separation of monodisperse Fe3O4 nanocrystals. Science. 2006; 314:964–967. [PubMed: 17095696]
52. Yean S, Cong L, Yavuz CT, Mayo JT, Yu WW, Kan AT, Colvin VL, Tomson MB. Effect of magnetite particle size on adsorption and desorption of arsenite and arsenate. J. Mater. Res. 2005; 20:3255–3264.
53. Chandra V, Park J, Chun Y, Lee JW, Hwang IC, Kim KS. Water-dispersible magnetite-reduced graphene oxide composites for arsenic removal. ACS Nano. 2010; 4:3979–3986. [PubMed: 20552997]
54. Raven KP, Jain A, Loeppert RH. Arsenite and arsenate adsorption on ferrihydrite: Kinetics, equilibrium, and adsorption envelopes. Environ. Sci. Technol. 1998; 32:344–349.
55. Morin G, Wang Y, Ona-Nguema G, Juillot F, Calas G, Menguy N, Aubry E, Bargar JR, Brown GE Jr. EXAFS and HRTEM evidence for As(III)-containing surface precipitates on nanocrystalline magnetite: implications for As sequestration. Langmuir. 2009; 25:9119–9128. [PubMed: 19601563]
56. Chakravarty R, Valdovinos HF, Chen F, Lewis CL, Ellison PA, Luo H, Meyerand ME, Nickles RJ, Cai W. Intrinsically Germanium-69 Labeled Iron Oxide Nanoparticle: Synthesis and In Vivo Dual-modality PET/MR Imaging. Adv Mater. 2014 Accepted.
57. Zeng J, Jia B, Qiao R, Wang C, Jing L, Wang F, Gao M. In situ 111In-doping for achieving biocompatible and non-leachable 111In-labeled Fe3O4 nanoparticles. Chem Commun (Camb). 2014; 50:2170–2172. [PubMed: 24430864]
58. Freund B, Tromsdorf UI, Bruns OT, Heine M, Giemsa A, Bartelt A, Salmen SC, Raabe N, Heeren J, Ittrich H, et al. A simple and widely applicable method to 59Fe-radiolabel monodisperse superparamagnetic iron oxide nanoparticles for in vivo quantification studies. ACS Nano. 2012; 6:7318–7325. [PubMed: 22793497]
59. Wong RM, Gilbert DA, Liu K, Louie AY. Rapid size-controlled synthesis of dextran-coated, 64Cu-doped iron oxide nanoparticles. ACS Nano. 2012; 6:3461–3467. [PubMed: 22417124]
60. Liu T, Shi S, Liang C, Shen S, Cheng L, Wang C, Song X, Goel S, Barnhart TE, Cai W, et al. Iron oxide decorated MoS2 nanosheets with double PEGylation for chelator-free radiolabeling and multimodal imaging guided photothermal therapy. ACS Nano. 2015; 9:950–960. [PubMed: 25562533]
61. Zhang Y, Hong H, Cai W. PET tracers based on Zirconium-89. Curr Radiopharm. 2011; 4:131–139. [PubMed: 22191652]
62. Holland JP, Divilov V, Bander NH, Smith-Jones PM, Larson SM, Lewis JS. 89Zr-DFO-J591 for immunoPET of prostate-specific membrane antigen expression in vivo. J Nucl Med. 2010; 51:1293–1300. [PubMed: 20660376]
63. Thorek DL, Ulmert D, Diop NF, Lupu ME, Doran MG, Huang R, Abou DS, Larson SM, Grimm J. Non-invasive mapping of deep-tissue lymph nodes in live animals using a multimodal PET/MRI nanoparticle. Nat Commun. 2014; 5:3097. [PubMed: 24445347]
64. Boros E, Bowen AM, Josephson L, Vasdev N, Holland JP. Chelate-free metal ion binding and heat-induced radiolabeling of iron oxide nanoparticles. Chemical Science. 2015; 6:225–236.
65. Choi HS, Liu W, Liu F, Nasr K, Misra P, Bawendi MG, Frangioni JV. Design considerations for tumour-targeted nanoparticles. Nat Nanotechnol. 2010; 5:42–47. [PubMed: 19893516]
66. Choi HS, Liu W, Misra P, Tanaka E, Zimmer JP, Itty Ipe B, Bawendi MG, Frangioni JV. Renal clearance of quantum dots. Nat Biotechnol. 2007; 25:1165–1170. [PubMed: 17891134]
67. Chen F, Ellison PA, Lewis CM, Hong H, Zhang Y, Shi S, Hernandez R, Meyerand ME, Barnhart TE, Cai W. Chelator-free synthesis of a dual-modality PET/MRI agent. Angew Chem Int Ed Engl. 2013; 52:13319–13323. [PubMed: 24166933]
68. Chakravarty R, Valdovinos HF, Chen F, Lewis CM, Ellison PA, Luo H, Meyerand ME, Nickles RJ, Cai W. Intrinsically germanium-69-labeled iron oxide nanoparticles: synthesis and in-vivo dual-modality PET/MR imaging. Adv Mater. 2014; 26:5119–5123. [PubMed: 24944166]

Further Reading/Resources

1. Sun X, Cai W, Chen X. Positron emission tomography imaging using radiolabeled inorganic nanomaterials. Acc Chem Res. 2015; 48:286–294. [PubMed: 25635467]
2. Lee DE, Koo H, Sun IC, Ryu JH, Kim K, Kwon IC. Multifunctional nanoparticles for multimodal imaging and theragnosis. Chem Soc Rev. 2012; 41:2656–2672. [PubMed: 22189429]
3. Lee N, Hyeon T. Designed synthesis of uniformly sized iron oxide nanoparticles for efficient magnetic resonance imaging contrast agents. Chem Soc Rev. 2012; 41:2575–2589. [PubMed: 22138852]
4. Mankoff DA. A definition of molecular imaging. J Nucl Med. 2007; 48:18N–21N.
5. Cai W, Chen X. Nanoplatforms for targeted molecular imaging in living subjects. Small. 2007; 3:1840–1854. [PubMed: 17943716]
6. Goel S, Chen F, Ehlerding EB, Cai W. Intrinsically radiolabeled nanoparticles: an emerging paradigm. Small. 2014; 10:3825–3830. [PubMed: 24978934]
7. Hong H, Zhang Y, Sun J, Cai W. Molecular imaging and therapy of cancer with radiolabeled nanoparticles. Nano Today. 2009; 4:399–413. [PubMed: 20161038]

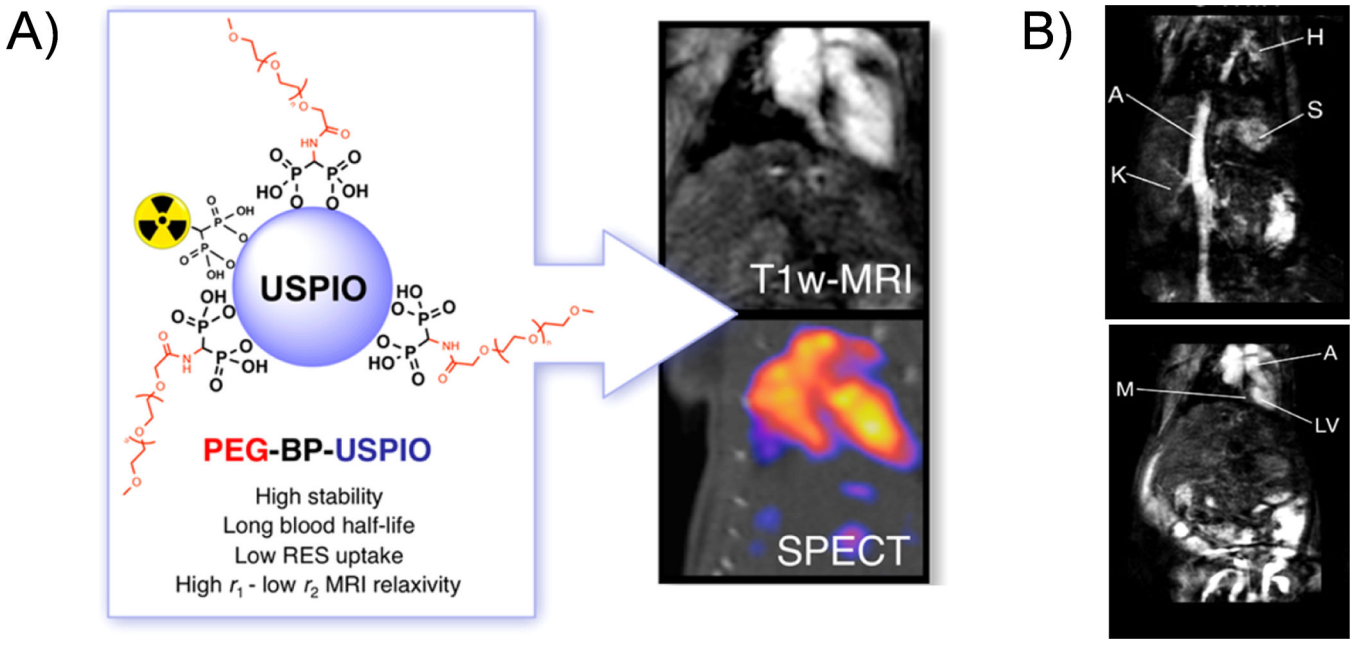

Figure 1.

(**A**) An illustration of SPECT/MRI multimodality imaging using ^{99m}Tc-PEG-BP-USPIO. (**B**) *In vivo* T_1-weighted MR imaging study on vessels (upper) and heart (down) of mice after injected with PEG(5)-BP-USPIO (Labels: H = heart, S = spleen, K = kidney, A =aorta, M = myocardium, LV = left ventricle. Reprinted with permission from [29].

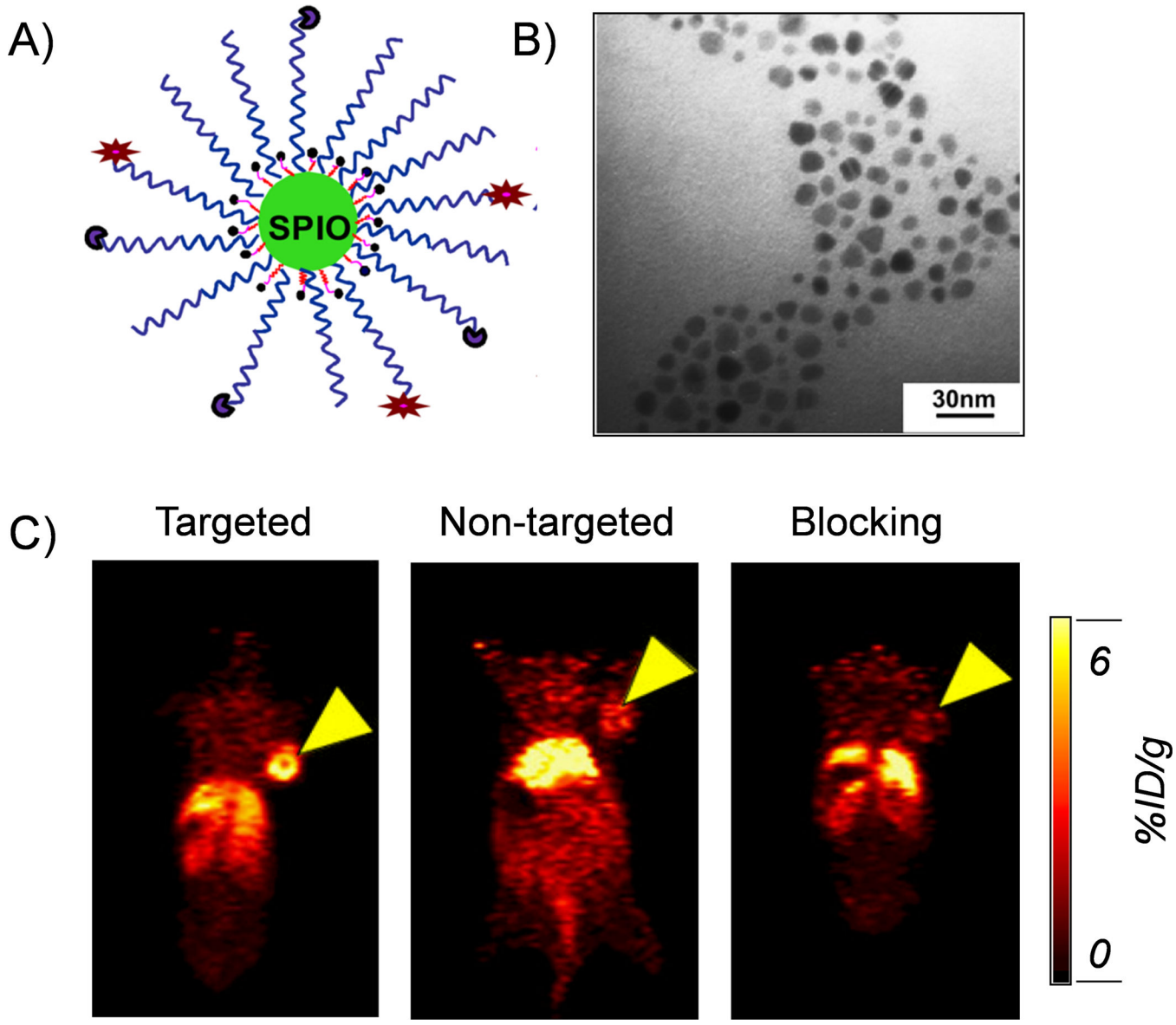

Figure 2.

(A) A schematic illustration of the ^{64}Cu-NOTA-IONP(DOX)-cRGD nanoconjugates for combined tumor-targeted drug delivery and PET/MRI imaging. (B) A TEM image of IONP(DOX)-cRGD. (C) *In vivo* PET images of U87MG tumor-bearing mice 24 h after injection of different nanoconjugates. From left to right: targeted group (^{64}Cu-NOTA-IONP-cRGD), non-targeted group (^{64}Cu-NOTA-IONP) and blocking group. Tumors were marked by yellow arrow-heads. Reprinted with permission from [41].

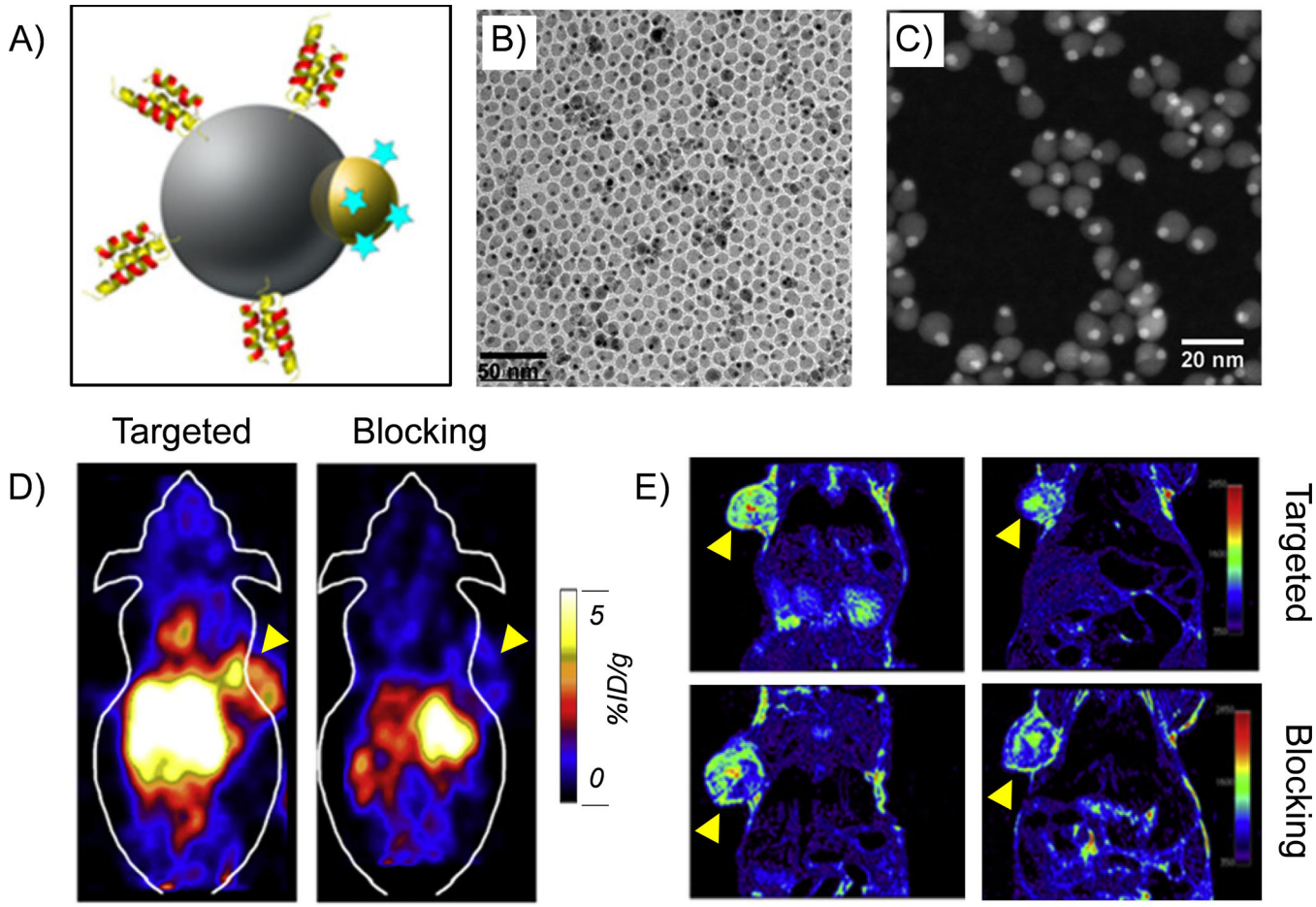

Figure 3.

(A) A schematic illustration of Au-IONP-Affibody. (B) A TEM image of Au-IONP. (C) A high-angle annular dark field image of Au-IONP. The Au nanoparticles were shown as the bright dots. (D) *In vivo* PET imaging of A431 tumor-bearing mice acquired 24 h after the injection of ^{64}Cu-NOTA-Au-IONP-Affibody. From left to right: targeted group and blocking group. (E) *In vivo* MR imaging of A431 tumor-bearing mice acquired 24 h after the injection of ^{64}Cu-NOTA-Au-IONP-Affibody. Tumors were marked by yellow arrow-heads. Reprinted with permission from [43].

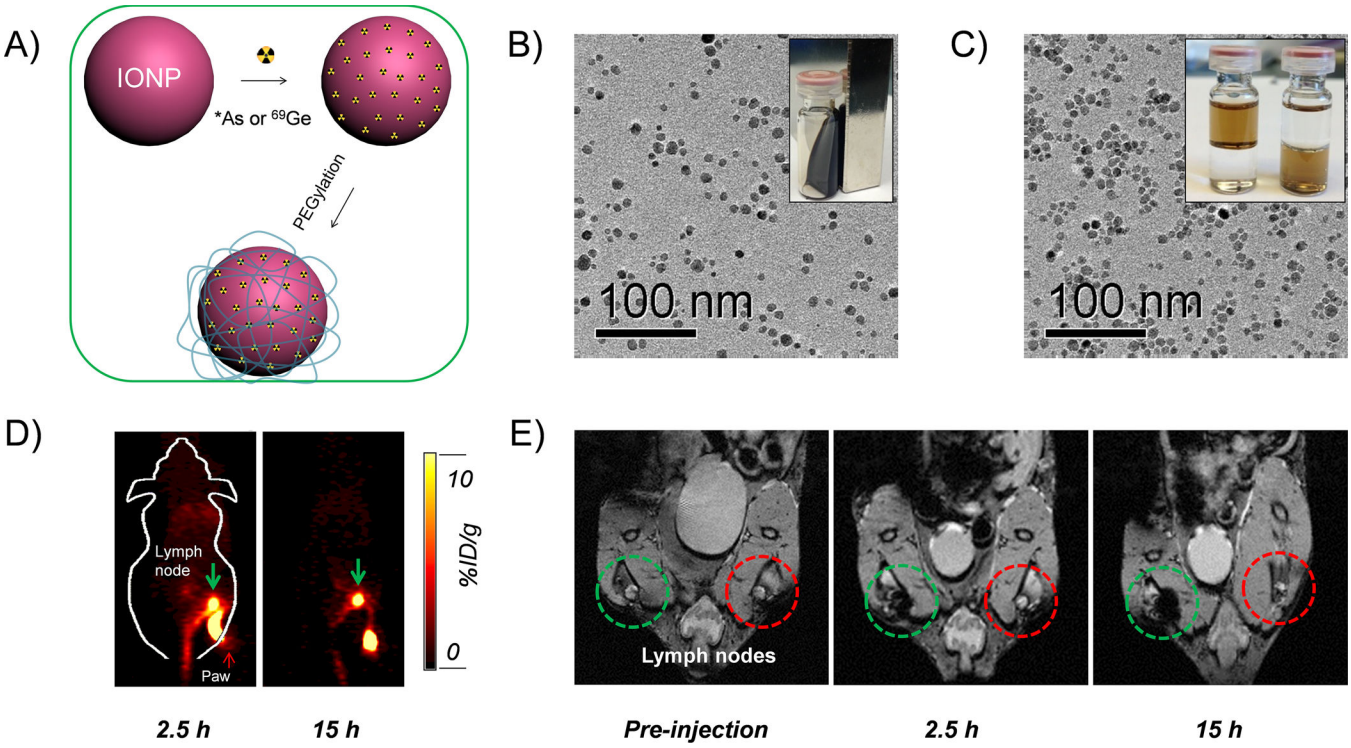

Figure 4.

(A) A schematic illustration of chelator-free synthesis of *As (or ^{69}Ge)-IONPPAA-PEG. (B) A TEM image of oleic acid capped IONPs. (C) A TEM image of PAA modified IONPs. (D) *In vivo* PET imaging of lymph nodes after the injection of *As-IONPPAA-PEG. (D) *In vivo* MR imaging of lymph nodes after the injection of *As-IONPPAA-PEG. Reprinted with permission from [67].

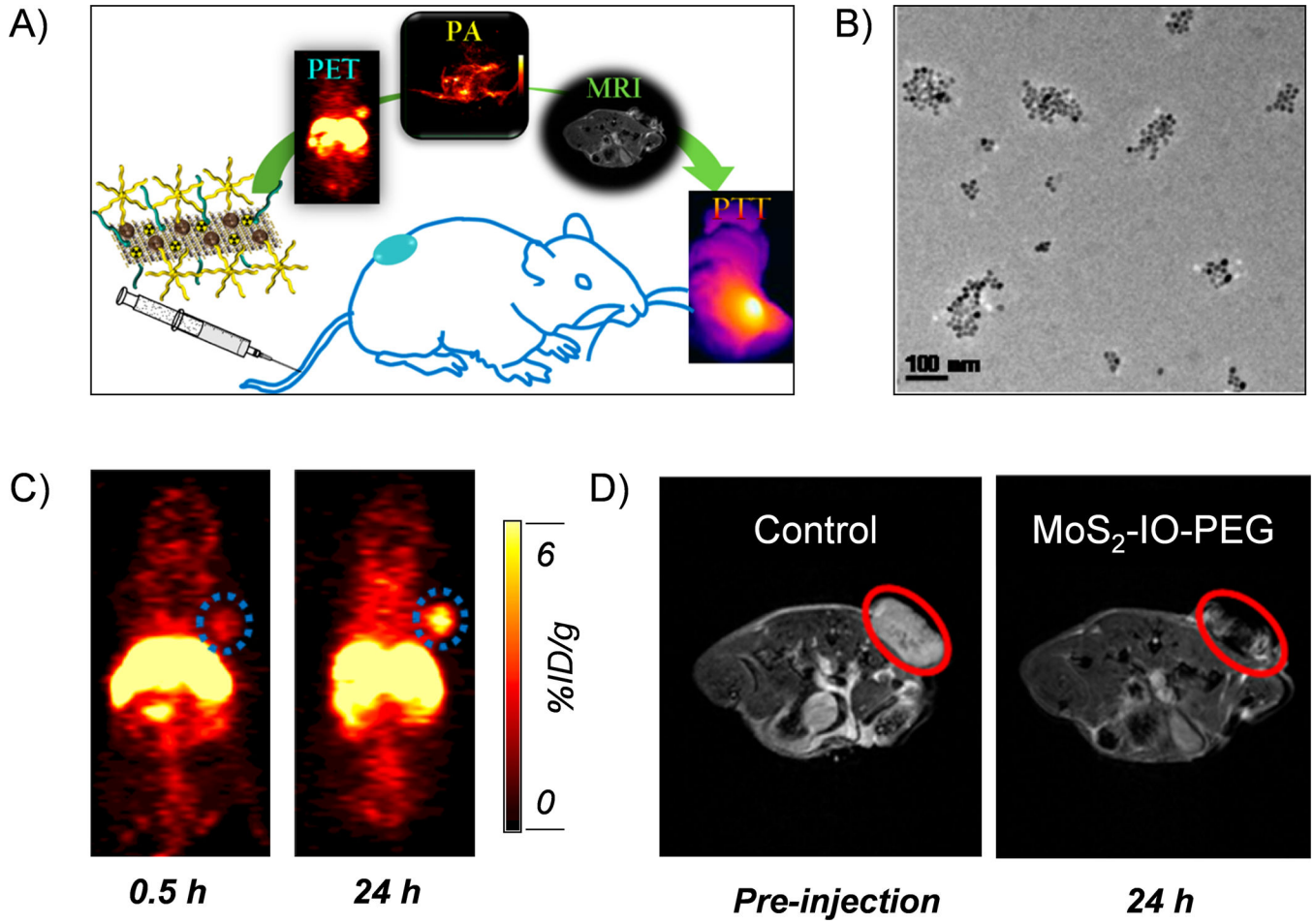

Figure 5.

(A) A schematic illustration of using ^{64}Cu-MoS_2-IONPs for multimodality image-guided photothermal therapy. (B) A TEM image of PEGylated MoS_2-IONPs. (C) PET imaging of 4T1 tumor-bearing mice after the injection of ^{64}Cu-MoS_2-IONPs. (D) MR imaging of 4T1 tumor-bearing mice after the injection of ^{64}Cu-MoS_2-IONPs. Reprinted with permission from [60].

Table 1

Representative examples of radiolabeled iron oxide nanoparticles

Radioisotopes	Half-life	Nanoparticles	Radiolabeling methods	Chelators	Applications	References
^{99m}Tc	6 h	IONPs-PEG	Chelator-free	N/A	SPECT/MRI	27
		IONPs-Poly(vinyl alcohol)	Chelator-based	DTPA, NOTA	SPECT/MRI	26
		USPIO	Chelator-based	Bisphosphonates	SPECT/MRI	28, 29
^{111}In	67.2 h	IONPs-dextran	Chelator-based	DTPA	SPECT/MRI	34
		IONPs-PEG	Chelator-free	N/A	N/A	57
		Ferumoxytol	Chelator-free	N/A	N/A	64
^{125}I	59 d	IONPs@SiO_2	Iodogen oxidization method	N/A	SPECT/MRI/Optical	37
^{68}Ga	68 min	INOPs	Chelator-based	NOTA	PET/MRI	44
^{18}F	109.8 min	Aminated cross-linked dextran IONPs	Click chemistry	N/A	PET/MRI	47
^{11}C	20.3 min	IONPs-NH_2 or IONPs-COOH	Methylation reactions	N/A	PET/MRI	49
^{64}Cu	12.7 h	IONPs-PEG	Chelator-based	DOTA	PET/MRI	39
		IONPs-dextran	Chelator-based	DOTA	N/A	40
		IONPs-PEG	Chelator-based	NOTA	PET/MRI	41
		MoS_2-IONPs	Chelator-free	N/A	PET/MRI	60
		Ferumoxytol	Chelator-free	N/A	N/A	64
^{89}Zr	3.3 d	Ferumoxytol	Chelator-based	DFO	PET/MRI	63
		Ferumoxytol	Chelator-free	N/A	PET/CT	64
^{69}Ge	69 h	IONPs@PAA	Chelator-free	N/A	PET/MRI	68
^{72}As	26 h	IONPs@PAA	Chelator-free	N/A	PET/MRI	67